Atmos. Meas. Tech. Discuss., doi:10.5194/amt-2016-118, 2016
Manuscript under review for journal Atmos. Meas. Tech.
Published: 26 July 2016

Atmospheric Measurement Techniques Discussions

Improved Methodologies for Continuous Flow Analysis of Stable Water Isotopes in Ice Cores

Tyler R. Jones[1], James W. C. White[2], Eric J. Steig [3], Bruce H. Vaughn [1], Valerie Morris [1], Vasileios Gkinis [4], Bradley R. Markle [3], Spruce W. Schoenemann [3]

[1] Institute of Arctic and Alpine Research, University of Colorado, Boulder, CO 80309-0450, USA
[2] Institute of Arctic and Alpine Research and Department of Geological Sciences, University of Colorado, Boulder, CO 80309-0450, USA
[3] Department of Earth and Space Sciences, University of Washington, Seattle, Washington 98195-1310, USA
[4] Centre for Ice and Climate, Niels Bohr Institute, University of Copenhagen, Denmark

Correspondence to: Tyler R. Jones (tyler.jones@colorado.edu)

Abstract. Water isotopes in ice cores are used as a climate proxy for local temperature and regional atmospheric circulation as well as evaporative conditions in moisture source regions. Traditional measurements of water isotopes have been achieved using magnetic sector isotope ratio mass spectrometry (IRMS). However, a number of recent studies have shown that laser absorption spectrometers (LAS) perform as well or better than IRMS. The new LAS technology has been combined with continuous flow analysis (CFA) to improve data density and sample throughput in numerous prior ice coring projects. Here, we present a comparable semi-automated LAS-CFA system for measuring high-resolution water isotopes of ice cores. We outline new methods for partitioning both system uncertainty and system mixing length into liquid and vapor components – useful measures for defining and improving the overall performance of the system. Critically, our methods take into account the uncertainty of depth registration that is not present in IRMS nor fully accounted for in other CFA studies. We also explain a method for introducing consecutive sections of isotopically distinct ice at the melt head to define the system-wide mixing length. These analyses are achieved using samples from a South Pole firn core, a Greenland ice core, and the WAIS Divide ice core. The measurement system utilizes a 16-position carousel contained in a freezer to consecutively deliver ~1m x 1.3cm^2 ice sticks to a temperature controlled melt head, where the ice is converted to a continuous liquid stream, and eventually vaporized using a concentric nebulizer for isotopic analysis. An integrated delivery system for water isotope standards is used for calibration to the VSMOW-SLAP scale and depth registration is achieved using a precise overhead laser distance device with an uncertainty of ± 0.2 mm. As an added check on our system, we perform inter-lab LAS comparisons using WAIS Divide ice samples, a corroboratory step not taken in prior CFA studies. The overall results are important for substantiating data obtained from LAS-CFA systems, including optimizing liquid and vapor mixing lengths, determining melt rates for ice cores with different accumulation and thinning histories, and removing system-wide mixing effects that are convolved with the natural diffusional signal that results primarily from water molecule diffusion in the firn column.

Atmos. Meas. Tech. Discuss., doi:10.5194/amt-2016-118, 2016
Manuscript under review for journal Atmos. Meas. Tech.
Published: 26 July 2016

Atmospheric Measurement Techniques Discussions

1 Introduction

The measurement of water isotopes in ice cores provides records of past hydrologic cycle variability (Dansgaard, 1964). The parameters δD and $\delta^{18}O$ are proxies for both local temperature and regional atmospheric circulation, while the second order parameter deuterium excess has been used to obtain information about source water evaporative conditions (temperature, humidity, and wind speed), as well as changes in the location of moisture source regions (Jouzel and Merlivat, 1984; Jouzel et al., 1997; Johnsen et al., 2001; Kavanaugh and Cuffey, 2003; Steig et al., 2013). These parameters have routinely been analyzed since the origins of ice core science, first in a precipitation experiment in Copenhagen in 1952, then on the visible layers of icebergs in the North Atlantic, and later in the Camp Century ice core (described in Dansgaard, 2005). Since these early experiments, a large collection of ice core water isotope records have been recovered from the Greenland Ice Sheet, the Antarctic Ice Sheet, and many high-latitude and/or high-altitude ice caps. These records have been instrumental in understanding climate change over annual to millennial timescales, including abrupt climate change events (Dansgaard et al., 1989; Grootes et al., 1993; and Alley, 2000), the bipolar see saw (WAIS Divide Project Members, 2015), and glacial-interglacial cycles (Petit et al., 1999).

Traditional measurements of water isotopes have been accomplished using customized prep-systems and isotope ratio mass spectrometry (IRMS; see a full list of abbreviations in Table 1). Typically, water samples are analyzed discretely using 3-5 cm intervals of ice. Isotopic ratios of oxygen are usually obtained using a CO_2/H_2O equilibration method (Epstein, 1953 and Craig et al., 1963). For hydrogen isotopes, a variety of methods have been used, including H_2/H_2O equilibration using a platinum catalyst and reduction of water with uranium, zinc or chromium (Bigelseisen et al., 1952; Bond, 1968; Coleman et al., 1982; Coplen, 1991; Vaughn et al., 1998; and Huber and Leuenberger, 2003).

Advances in high-precision laser absorption spectroscopy (LAS) methods are now widely adopted as an alternative to IRMS methods (Kerstel et al., 1999; Lis et al, 2008; Gupta, et al, 2009; and Brand et al., 2009). There are currently two main LAS methods used: cavity ring-down laser spectroscopy (CRDS; manufactured by Picarro, Inc.) and off-axis integrated cavity output laser spectroscopy (OA-ICOS; manufactured by Los Gatos Research). The CRDS method (utilized in this study) requires the input of water vapor into a detection cavity that confines and reflects laser pulses using a series of mirrors. By comparing the extinction of a laser pulse at different frequencies in an empty cavity and in a cavity filled with water vapor, water isotope concentrations can be determined (Crosson, 2008).

Systems have been developed that continuously deliver water vapor into LAS measurement devices. The technique, known as continuous flow analysis (CFA), is accomplished by slowly melting a solid ice stick into a continuous liquid stream, which is then vaporized and injected into the LAS instrument. CFA has been widely used for chemical measurements in ice cores (e.g. Rothlesberger, 2000; Osterberg et al., 2006; Bigler et al., 2011; and Rhodes et al., 2013). Other works by Huber

Atmos. Meas. Tech. Discuss., doi:10.5194/amt-2016-118, 2016
Manuscript under review for journal Atmos. Meas. Tech.
Published: 26 July 2016

Atmospheric Measurement Techniques Discussions

and Leuenberger (2005) and Gkinis et al. (2010; 2011) established the CFA framework for water isotope analysis. In particular, Gkinis reproduced traditional IRMS water isotope measurements in Greenland ice using a Picarro L1102-*i* CRDS instrument. Gkinis found that the precision of hydrogen isotope measurements was comparable to IRMS, while oxygen isotope precision was slightly decreased. Substantial increases in depth resolution and shorter analysis time were realized. Maselli et al. (2012) expanded on Gkinis' technique by testing multiple new-generation Picarro devices (L2120-*i* and L2130-*i*) and found similar results. Later, Emanuelsson et al. (2015) used OA-ICOS to continuously analyze water samples from an ice core, achieving reductions in isotopic step-change response time and memory effects.

1.1 Goals of this Study

In this study, we present a semi-automated water isotope CRDS-CFA system developed at the Institute of Arctic and Alpine Research (INSTAAR) Stable Isotope Lab (SIL). We analyze δD, $\delta^{18}O$, and deuterium excess values in a series of ice samples from Greenland and Antarctica. New methods are used to test the uncertainty of the isotopic data. We propose a system uncertainty test using replicate ice to account for multiple sources of uncertainty on the CRDS-CFA system. We then present steps to create isotopically distinct ice sticks to evaluate the impulse response of the system, which yields a CFA system mixing length. The mixing length is a measure of 1σ displacement of water molecules from their original position in the solid ice sample. This is important for two reasons: 1) The system mixing length needs to be distinguished from the effects of diffusion occurring naturally in the ice sheet and 2) based on the mixing length, system flow rates can be adjusted to prevent isotopic signal attenuation in low accumulation ice core sites. Based on the system wide mixing length, we propose a way to separate isotopic mixing effects in the liquid and vapor phase. This test is important for CFA systems that have complicated liquid phase components, such as those systems analyzing multiple chemical species that require extra lengths of tubing to transport liquid water. We then perform inter-lab and inter-system isotopic testing of firn ice and deep ice. Due to decreased density, firn ice has been difficult to measure on other CFA systems. Despite our best efforts, we recommend that low-density firn column samples be analyzed discretely. However, if the firn ice is allowed to sinter for an extended period during storage, this greatly aids in CFA measurement. The results of this study will be used in the analysis of the WAIS Divide ice core (WDC), the South Pole ice core (SPICE), and other ice cores in the future.

Atmos. Meas. Tech. Discuss., doi:10.5194/amt-2016-118, 2016
Manuscript under review for journal Atmos. Meas. Tech.
Published: 26 July 2016

Atmospheric Measurement Techniques Discussions

2 Data and Methods

2.1 Water Isotope Measurements

The ratio of heavy to light water isotopes in a water sample is expressed in delta notation (Epstein, 1953; Mook, 2000) relative to Vienna Standard Mean Ocean Water (VSMOW, 0.00‰) and normalized to Standard Light Antarctic Precipitation (SLAP, -55.5‰ relative to VSMOW):

$$\delta_{sample} = \left[\left(\frac{R_{sample}}{R_{VSMOW}}\right) - 1\right] \quad (1)$$

where R is the isotopic ratio $^{18}O/^{16}O$, $^{17}O/^{16}O$, or D/H (i.e. $^{2}H/^{1}H$) in the sample or VSMOW. The δ values ($\delta^{18}O$, $\delta^{17}O$, or δD) are thus deviations from VSMOW, usually expressed in parts per thousand (per mil or ‰). The deuterium excess parameter (dxs) is defined as function of both hydrogen and oxygen isotope ratios:

$$\text{dxs} = \delta D - 8 \cdot \delta^{18}O \quad (2)$$

The precise measurement of dxs (‰) has historically been challenging because IRMS methodology requires that oxygen and hydrogen water isotope ratios be analyzed on separate systems, which increases uncertainty. The CRDS-CFA technique removes multi-system uncertainty because both isotopic values are measured simultaneously on a single sample with the same system.

2.2 Experimental System

The CRDS-CFA system is composed of three parts: 1) The ice core melting component, 2) the liquid-to-gas conversion component, and 3) the isotopic analyzer. A full system schematic is shown in Figure 1. The ice core melting component can accommodate 16 sticks of ice that measure ~1m x 1.3cm^2 (each stored in 1.9 cm^2 acrylic tubes) that are loaded vertically into a rotating carousel contained in a freezer. Using a computer-controlled stepper motor (Parker ViX), the carousel rotates individual ice sticks over an aluminum melt head. The melt head (51 mm^2 x 12.6 mm) is machined with 2 mm concentric square catchments that channel melt water into a small drain. To regulate temperature, the melt head is bolted with thermal paste to a heater block (51 mm^2 x 45.8 mm) that is maintained at 14.6 ± 0.1 °C by internally circulating dilute propylene glycol from a temperature-controlled bath. This method is preferable to proportional-integral-derivative controlled resistive heaters used in most systems, which introduce small temperature fluctuations that can result in varying melt rates. At 14.6°C, the 13mm^2 ice sticks typically melt at an average rate of 2.5 cm/min. This melt rate can be increased or decreased by changing the temperature of the melt head.

Atmos. Meas. Tech. Discuss., doi:10.5194/amt-2016-118, 2016
Manuscript under review for journal Atmos. Meas. Tech.
Published: 26 July 2016

Atmospheric Measurement Techniques Discussions

For the liquid-to-gas conversion component of the system, liquid water is drawn away from the melt head interface using peristaltic pumps (Masterflex L/S 7534-04). Liquid water from the outer square catchment of the melt head is collected for use as isotopic water standards. The inner square catchment is pumped at a rate matching that of the ice stick melt. This liquid water is pushed through an 8-micrometer disposable filter backed by a 10-micrometer Peek frit (IDEX A-411). With filters in place, the system is tolerant of ice with ash or dust layers.

The filtered water then enters a 2 ml glass, open-top vial where bubbles can escape (debubbler). A portion of the debubbled water is used as primary flow (i.e. for isotopic measurements), which is aspirated from the debubbler through a 1/16" OD 0.020" ID tubing via a selector valve (VICI Cheminert 10P-0392L). The water is then channeled through a Valco 6-port stream selection valve (Valco Instruments, Co. Inc.). To induce suction, high-pressure (80 psi) dry air is supplied to a downstream glass concentric nebulizer (Meinhard TL-HEN-150-A0.1), which creates a pressure difference that pulls the primary water out of the debubbler, through the Valco selection valve, and out of the nebulizer. The nebulizer converts the primary liquid water into a fine spray with a nominal droplet size of ~1.5 micrometers. The spray is directed into a 20.0 x 1.8 cm Pyrex vaporizing tube that is heated to 200 °C inside a ceramic tube furnace (Whatlow VC400N06A). Additional dry air (< 30 ppm H_2O) is added at a rate of ~3.5 L/min to dilute the water vapor and achieve a final water vapor content of ~25,000 ppm H_2O, which is within the optimal range of 20,000-40,000 ppm H_2O for the Picarro L2130-*i*. Finally, the water vapor flows through an intake line (3.175 mm OD x 2 mm ID x 10 cm stainless steel tubing) inserted approximately 5 cm into the Pyrex vaporizing tube. This line is plumbed into a Picarro L2130-*i* analyzer by an open split interface. Any excess vapor is vented away from the instrumentation.

At the Valco 6-port stream selection valve, the primary water flow can be switched off, allowing another auxiliary port to be switched on. Each auxiliary port is connected to 30 ml glass vials of secondary isotopic water standards, which can be analyzed and used for calibration of ice core measurements to international reporting standards. The auxiliary port water is pulled in the same fashion as the primary flow by suction induced by the nebulizer. Additional water streams (secondary flow) are pumped from the debubbler to an electrical conductivity (EC) measurement cell (Amber Science 1056) and to a fraction collector (Gilson 215). The EC measurement allows for the comparison of chemical signatures at a known depth between labs. The fraction collector is used to archive water samples for discrete analysis and as a safeguard against system failures. It is programmed to fill approximately twenty-five 2 ml glass vials for every meter of ice melted, approximating a discrete ice sampling resolution of about 2.5 cm.

It should be noted that transforming the liquid water stream to vapor can be accomplished in different ways. Previous CFA isotopic systems have accomplished this by pumping liquid water through a ~100 μm ID quartz capillary to a Swagelok Tee that acts as an open split (Gkinis et al. 2010; 2011). This method has the advantage of simplicity, but relies heavily on

Atmos. Meas. Tech. Discuss., doi:10.5194/amt-2016-118, 2016
Manuscript under review for journal Atmos. Meas. Tech.
Published: 26 July 2016

precise placement of the capillary within the tee fitting. Alternatively, using a nebulizer as per Emanuelsson et al. (2015) provides stability water vapor concentrations within the CRDS vapor cavity. There are also fewer issues with system clogging. When clogs did occur in the nebulizer, they were easily identified and cleaned by back flushing the nebulizer using a vacuum.

2.3 A Typical Analysis Day

On a given run day, we perform a sequence of measurements related to calibration and correction (Figure 2). At the beginning and end of a melt day, secondary isotopic water standards are analyzed to calibrate the ice core data against International Atomic Energy Agency (IAEA) primary standards (VSMOW2, SLAP2, and GISP). We use four secondary standards including Boulder Standard Water (BSW), Antarctic Standard Water (ASW), Greenland Standard Water (GSW), and Polar Standard Water (PSW). Each secondary standard is analyzed twice for 20 minutes at the beginning and end of the day (4 times total), except for PSW, which is analyzed only 2 times total. Table 2 contains a summary of isotopic standards.

To characterize isotopic mixing throughout the system, three small (20 cm x 13mm^2) sections of laboratory prepared ice are made from batches of isotopically distinct waters with δD values of -240 ‰ for the 1st and 3rd sections and -120 ‰ for the 2nd section (hereafter referred to as mock ice). The mock ice is created by filling lay-flat tubing with isotopically homogenous water, freezing the water at -60 °C in chilled ethanol to minimize fractionation, and cutting the ice into small sections using a band saw. We found that a temperature of -30 °C produced the least amount of fractionation, but that fractionation during the freezing process prevented the mock ice from being used as strict isotopic standards. The mock ice is analyzed twice per day at the beginning and end of an ice core melt sequence. Each instance of mock ice analysis is used to determine how the CRDS-CFA system is responding to an instantaneous step change in isotopic values (in this case, a change from -240 to -120 ‰, and vice versa). Ideally, the system would instantly register the change, but mixing in the liquid and vapor phase causes a slower reaction. This mixing effect can be quantified using transfer and impulse functions.

An ice core melt sequence occurs in between analysis of secondary isotopic water standards and mock ice. Key variables are closely monitored during this time, including water concentration in the Picarro instrument, the melt rate, and depth registration. During the ice core melt sequence, every set of four ice cores is separated by 20 cm sections of isotopically homogenous ice with a δD value of about -115‰ (hereafter referred to as push ice). The push ice isotopic value is much heavier than the surrounding ice core samples to ensure that they can be easily distinguished from each other. The push ice also maintains a consistent thermal load on the melt head and consistent water vapor delivery to the Picarro during routine maintenance tasks that include changing the filters and cleaning the melt head.

Atmos. Meas. Tech. Discuss., doi:10.5194/amt-2016-118, 2016
Manuscript under review for journal Atmos. Meas. Tech.
Published: 26 July 2016

Atmospheric Measurement Techniques Discussions

2.4 System Software

A graphical user interface (GUI) developed in Python is used to automate and record many of the procedures related to carousel positioning, active Valco port, ice core depth registration, quality control (e.g. water level in the debubbler and melt rate), electrical conductivity, and commenting. This auxiliary data, along with the data collected from the Picarro instrument, are collected using a serial port (MOXA UPORT 1610-8). All data are recorded at the same data frequency as the isotopic data generated by the Picarro L2130-*i*, and the data are exported as a raw text file generated by the Picarro and GUI. The raw data are then post-processed off-line by a separate semi-automated Python script.

During post-measurement data analysis, we first identify and separate various analysis sections (e.g. secondary standards, mock ice, push ice, and ice cores) using integer values in a comment field (e.g. mock ice section are commented '159' while ice core sections are commented '175'). Depth data for the ice core sections (derived from the distance laser) are filtered for any outliers. This may arise when an ice stick temporarily wedges against the acrylic tube during ice melt. The top section of the ice remains stationary, while the bottom continues to melt. In the depth registration field, this appears as a flat line followed by an abrupt increase in depth (usually not longer than 15 seconds). These sections are interpolated across to characterize the depth of the accompanying isotopic measurements. Ice-wedging can be largely eliminated by fitting a set of small vibrating devices made from DC motors with off-axis weight to the outside of the acrylic tubes, where vibrational frequency is controlled by a variable DC power supply. For every ice core section preceded by push ice, we assign an initial depth to the ice core section at the minimum derivative of the isotopic step-change. This effectively marks the mid-point of the isotopic step change and corresponds to the point when ice core isotopic values begin to dominate the preceding push ice signal. The depth assignment scheme can be tested and verified using discrete samples of the same ice section.

The large amount of data generated by CRDS-CFA requires a different approach to data handling than IRMS. The Picarro L2130-*i* generates and records isotopic data at approximately ~1.18 Hz intervals (0.85 second intervals). For a melt rate of 2.5 cm/min, this translates into sub-millimeter isotopic resolution, and roughly 2,800 data points per meter. At 12 meters of ice core per day, and recording 36 total quality control parameters, each melt day generates over 1.2 million data points. For a deep ice core of ~3,000 meters, this equates to ~300 million data points recovered in the course of 250 melt days. In comparison, traditional IRMS produces about ~60 ice core data points per day, equating to the analysis of ~2.0 meters of ice per day at 3.0 cm resolution. For a deep ice core of ~3,000 meters, this would generate a total of 99,000 data points for a single parameter and require about 1,500 analysis days to complete. The CRDS-CFA system presented here provides a ~6 fold time-savings and an order of magnitude improvement in data density compared to traditional IRMS methods. However, to process the CRDS-CFA data requires multiple computer processors, and for the largest tasks, super-computing can reduce processing times from hours or days to minutes.

Atmos. Meas. Tech. Discuss., doi:10.5194/amt-2016-118, 2016
Manuscript under review for journal Atmos. Meas. Tech.
Published: 26 July 2016

Atmospheric Measurement Techniques Discussions

2.5 System Performance

The protocol used for the correction of measured water isotope values to the VSMOW-VSLAP scale is performed at the beginning and end of a melt day using secondary isotopic standards (i.e. BSW, ASW, GSW, and PSW). These secondary isotopic standards are calibrated to the VSMOW-SLAP scale based on measurements of the primary standards VSMOW2 and SLAP2 (Lin et al., 2010). To perform the correction, we first isolate the last 5 minutes (out of 20 minutes total) of each secondary standard run. Each standard is run four times per day, except PSW, which is only analyzed twice. We then take the average of the isolated 5-minute sections for each standard. We now have a single averaged value for BSW, ASW, GSW, and PSW. The BSW, ASW, and PSW are assigned as "measured" values, which are plotted versus their "known" VSMOW-SLAP calibrated values. We then correct the GSW isotopic standard using the following equation:

$$x_{corrected} = \frac{y_{measured} - b_{calibrated}}{m_{calibrated}} \quad (3)$$

where $y_{measured}$ is the averaged GSW value (as described above) measured on the CRDS-CFA system, $b_{calibrated}$ is the y-intercept of the linear regression, $m_{calibrated}$ is the slope of the linear regression, and $x_{corrected}$ is the GSW value calibrated to the VSMOW-SLAP scale. This same calibration is done for all ice core isotopic measurements.

We also use the secondary isotopic standards to define internal precision and accuracy of the CRDS-CFA system. The internal precision is determined by taking the average standard deviation of each of the last 5 minutes of each 20-minute secondary standard run, while the accuracy is defined as the difference of the measured GSW value from its known value. These values can then be compared over the long-term to monitor the performance of the CRDS-CFA system. The average internal precision (1σ) and average accuracy for δD was 0.49 and 0.39 ‰, respectively. For $\delta^{18}O$, these values were 0.05 and 0.01 ‰, respectively. We note that there is no universally accepted method for defining internal precision and accuracy in water isotope CFA systems. For example, Gkinis (2010; 2011) used only 3 secondary isotopic standards, whereas we use four. This should be taken into account when comparing internal precision and accuracy across different CFA papers.

The stability of the Picarro CRDS analyzer is determined by tests of Allan variance (Allan, 1966), which provides a measure of the intrinsic noise in a measurement system as a function of the integration time (i.e. the amount of time a parcel of vapor is present in the laser cavity). The Allan variance is defined as:

$$\mathrm{AVAR}^2(\tau) = \frac{1}{2(n-1)} \sum_{i=1}^{n-1} (y(\tau)_{i+1} - y(\tau)_i)^2 \quad (4)$$

where τ is the integration time, $y(\tau)$ is the average value of the measurements in an integration bin of length τ, n is the total number of bins, and AVAR is the Allan variance. The idea of integration bins simply refers to taking a long sequence of data

Atmos. Meas. Tech. Discuss., doi:10.5194/amt-2016-118, 2016
Manuscript under review for journal Atmos. Meas. Tech.
Published: 26 July 2016

Atmospheric Measurement Techniques Discussions

and dividing it into smaller successive bins of a certain averaging time τ, and then averaging the values in each bin to determine values for $y(\tau)$.

We determine Allan deviation (the square root of Allan variance) by continuous injection of isotopically homogenous water into the CRDS-CFA for many hours at a time. The Allan deviation values for a 7-hour run are plotted in Figure 3 and selected Allan deviation values are shown in Table 3. The Allan deviation shows that the CRDS-CFA system short-term noise is negligible (i.e. 0.1‰ in δD for a 10-second integration time; a small value compared to the isotopic signal seen in ice cores), that the system is most stable at integration time values of 1000 seconds or greater, and that the system is stable over all integration times to at least 3 hours in length. We provide a direct estimate of system uncertainty on CRDS-CFA isotopic measurements later in this paper.

2.6 Isotopic Step-Change Correction

During a typical analysis day, every 4th ice core stick is separated by isotopically distinct push ice. Ideally, the isotopic shift between push ice and the beginning of an ice core stick would occur instantaneously. However, mixing effects in the CRDS-CFA system result in a smoothed transition. Possible contributors to the mixing effect include: liquid mixing in tubing and the debubbler, liquid drag on tubing walls, vapor mixing after the nebulizer, vapor interactions with two Picarro instrument filters (Mykrolis Wafergaurd) prior to entering the laser cavity, adsorption of water molecules onto the laser cavity walls, and diffusional effects (probably negligible) that can occur at any point in the CRDS-CFA system. In laboratory tests, we note that removal of the 1st Picarro instrument filter can reduce mixing in the vapor phase by 40%. However, the removal of the filter also risks damaging the laser cavity, and we chose to leave the filter in place.

Mixing during an isotopic step-change causes smoothing in the first ~5-7 cm of an ice core sample. This effect can be partially corrected for by using a mixing correction, achieved by quantifying mixing coefficients (c_t) during a mock ice δD isotopic shift from -240 to -120 ‰. For example, at a time of 5 seconds after a shift in mock ice at the melt head, the measured isotopic value (not including the delay in transport from the melt head to the CRDS instrument) may only be 2% of the expected value. After 40 seconds, the measured value may be 40% of the expected value, and after 100 seconds, the measured value may be 95% of the expected value. For these three examples, the mixing coefficients would be 0.02, 0.40, and 0.95, respectively. To remove noise from the c_t calculation, we average mock ice isotopic values, normalize between 0 and 1, and apply a cubic spline. The water isotope mixing correction is described by equation 4 of Vaughn et al. (1998):

$$\delta_{mc} = \frac{\delta_m - \delta_{mp}(1 - c_t)}{c_t} \quad (5)$$

where δ_m is the measured isotopic value at time t, δ_{mp} is the previously measured isotopic value at time $t-1$, c_t is the memory coefficient at time t, and δ_{mc} is the corrected isotopic value at time t. An example of an isotopic mixing correction

Atmos. Meas. Tech. Discuss., doi:10.5194/amt-2016-118, 2016
Manuscript under review for journal Atmos. Meas. Tech.
Published: 26 July 2016

is shown in Figure 4. We find that the mixing correction can only be applied at $c_t \geq 0.65$ due to inconsistencies in the timing of the isotopic transition related to small perturbations in flow rate, which become amplified in the mixing correction at small c_t. For $c_t \geq 0.65$, the correction saves an additional ~2.25-3.15 cm of data that would otherwise be discarded. For a typical deep ice core of 3000 m, there are 750 step-changes (every 4th ice core stick). This correction saves ~16.9 – 23.7 m of isotopic data. In the data output file we produce, the depths of mixing corrections are flagged so researchers can decide whether to include these data in their calculations.

2.7 Mixing Length Calculations

A transfer function and impulse response function of the system can be defined using mock ice or secondary water standards. The transfer function is the system response to an instantaneous isotopic step-change at the melt head or Valco stream selection valve. The impulse response function is the first derivative of the transfer function. The standard deviation of the impulse response corresponds to the mixing length (often referred to as diffusion length in other publications), which defines the average movement of a water molecule in the time or depth domain relative to its original position in the ice sample or within a vial of water (i.e. input from secondary isotopic standards). Figure 5 shows transfer functions and impulse response functions of the CRDS-CFA system for δD and $\delta^{18}O$.

In previous work by Gkinis et al. (2010, 2011), a transfer function is fit to an isotopic step change using a scaled version of the cumulative distribution function (CDF) of a normal distribution described by:

$$\delta_{model}(z) = \frac{C_1'}{2}\left[1 + erf\left(\frac{t - t_o}{\sigma_n\sqrt{2}}\right)\right] + C_2' \quad (6)$$

where C_1' and C_2' are isotopic step change values, t the time, t_o the initial time, and σ_n is the standard deviation (i.e. the mixing length) – all of which are estimated by least squares optimization. The impulse response of the system is described by a Gaussian:

$$G_n(z) = \frac{1}{\sigma_n\sqrt{2\pi}} e^{-\frac{t^2}{2\sigma_n^2}} \quad (7)$$

We modify this approach because the system response to an isotopic step change is skewed (see Figure 5). We instead fit a transfer function in the form of a log-normal CDF multiplied with a log-normal CDF (log-log fit):

$$\delta_{model}(z) = \frac{1}{2}\left[1 + erf\left(\frac{t - t_1}{\sigma_1\sqrt{2}}\right)\right] \cdot \frac{1}{2}\left[1 + erf\left(\frac{t - t_2}{\sigma_2\sqrt{2}}\right)\right] \quad (8)$$

where z_1, z_2, σ_1, and σ_2 are predetermined to maximize the fit. The impulse response function is found by fitting a skew

Atmos. Meas. Tech. Discuss., doi:10.5194/amt-2016-118, 2016
Manuscript under review for journal Atmos. Meas. Tech.
Published: 26 July 2016

Atmospheric Measurement Techniques Discussions

normal probability density function (Azzalini and Valle, 1996) to the first derivative of the log-log transfer function:

$$\delta_{model}(z) = 2\phi(x)\Phi(\alpha x) \quad (9)$$

where $\phi(x)$ is the standard normal PDF, $\Phi(x)$ is the standard normal CDF, and α is a shape parameter. The transform $x \rightarrow \frac{x-\varepsilon}{\omega}$ introduces the location parameter ε and the scale parameter ω. The mixing length term σ_s is then recovered by:

$$\beta = \frac{\alpha}{\sqrt{1+\alpha^2}} \quad (10)$$

$$\sigma_s^2 = \omega^2\left(1 - \frac{2\beta^2}{\pi}\right) \quad (11)$$

where α, ε, and ω are estimated by least squares optimization.

The difference in mixing lengths between water originating from ice sticks at the melt or from secondary isotopic standards at the Valco valve is useful for partitioning mixing effects in the liquid and vapor phase of the CRDS-CFA system. Solid ice mixing lengths ($\sigma_{mock\ ice}$; determined from mock ice step changes) characterize mixing in the entire CRDS-CFA system, including the melt head, tubing, debubbler, nebulizer, Pyrex furnace tube, and laser cavity. Conversely, secondary isotopic standards mixing lengths (σ_{SWS}; determined from secondary isotopic standard step changes) characterize mixing primarily in the vapor phase because the liquid tubing pathway from the Valco stream selector valve to the nebulizer and furnace (where liquid water is converted to vapor) is short.

Using equations 6-11, mixing length values can be determined for $\sigma_{mock\ ice}$ and σ_{SWS} (Table 4), where the difference in quadrature between the two is the amount of mixing occurring in the liquid phase (σ_{LQD}) of the CRDS-CFA system. We find that the majority of the mixing in our CRDS-CFA system occurs in the liquid phase (i.e. downstream of the melt head to the Valco stream selection valve), while the remainder occurs in the vapor phase of the system (i.e. downstream of the Valco stream selection valve to the laser cavity).

The $\sigma_{mock\ ice}$ can also be thought of as the full CRDS-CFA system mixing length. This value is important for determining key parameters related to the performance of the system. For example, if a series of ice core samples have an average layer thickness of ~23.0 cm/year (a typical value at ~200 m depth in the WAIS Divide ice core), then a $\sigma_{mock\ ice}$ value of ~1 cm would have almost no affect on the attenuation of the natural signal. However, if the average layer thickness was ~2.0 cm/year (a typical value for very low accumulation sites in East Antarctica), then $\sigma_{mock\ ice}$ = ~1 cm would have a large

Atmos. Meas. Tech. Discuss., doi:10.5194/amt-2016-118, 2016
Manuscript under review for journal Atmos. Meas. Tech.
Published: 26 July 2016

Atmospheric Measurement Techniques Discussions

attenuation affect on the isotopic signal. For low accumulation sites, it would be necessary to significantly decrease the flow rate of a CRDS-CFA system when measuring ice cores, as this will decrease the $\sigma_{mock\ ice}$ values. Figure 6 shows a comparison of $\sigma_{mock\ ice}$ for the CRDS-CFA system vs. a typical diffusion length occurring naturally from diffusional processes in the Antarctic ice sheet at the location of the WAIS Divide ice core. In our data output file, values of $\sigma_{mock\ ice}$ and flow rate are included for all depths to allow for CRDS-CFA mixing corrections, and for comparison to diffusion occurring naturally in an ice sheet.

3 Results and Discussion

3.1 Greenland Test Ice

To test CRDS-CFA external precision (also known as repeatability), nine sticks of ice were cut from a single meter of Greenland test ice (GTI) at about 400 meters depth, obtained from the National Science Foundation National Ice Core Laboratory (Lakewood, Colorado). This ice was a byproduct of initial tests of the U.S. Deep Ice Sheet Coring Drill performed in Greenland in 2006 (Johnson et al., 2007). The same drill was deployed in West Antarctica to obtain the WAIS Divide ice core. Seven of the nine GTI sticks were analyzed on the CRDS-CFA system, three of which were broken into parts to test our depth registration methodology. The final two GTI sticks were discretely sampled at 1 cm and 5 cm increments, melted into vials, and analyzed on a separate Picarro L2130-*i*.

The isotopic data for the seven 1-meter long GTI sticks analyzed on the CRDS-CFA system was measured at sub-millimeter resolution to determine external precision. These data were then averaged to 1 cm successive values (GTI-1cm) for each stick, resulting in seven values at each 1 cm increment, from which a standard deviation was determined. This resulted in a total of 100 standard deviation values, and the mean of these values is used to estimate the CRDS-CFA system uncertainty (Figure 7). This approach gives a combined estimate of the analytical uncertainty on the CRDS isotope measurement, plus additional uncertainty introduced in the depth registration process for each ice stick. We find system uncertainty values (1σ) for δD, $\delta^{18}O$, and dxs of 0.55, 0.09, and 0.55 ‰, respectively. For comparison, traditional IRMS measurements for δD, $\delta^{18}O$, and dxs are commonly reported with uncertainties of about 1.0 0.1, and 1.3 ‰, respectively.

CRDS-CFA system uncertainty can be subdivided into two parts: uncertainty arising on the preparation side of the system (i.e. uncertainty occurring prior to vapor entering the CRDS instrument) and uncertainty arising on the CRDS side of the system (i.e. uncertainty occurring in the laser cavity and during isotopic analysis). We can isolate the CRDS uncertainty by analyzing a continuous stream of isotopically homogenous water (IHW) inputted directly into the CRDS instrument. We take averages of the IHW over consecutive 24-second intervals (supplement), which correspond to the time needed to melt 1 cm of ice at a melt rate of 2.5 cm/min. The standard deviation of 100 consecutive 24-second averages of the IHW (the

Atmos. Meas. Tech. Discuss., doi:10.5194/amt-2016-118, 2016
Manuscript under review for journal Atmos. Meas. Tech.
Published: 26 July 2016

Atmospheric Measurement Techniques Discussions

equivalent of a meter long section of ice) yields the CRDS uncertainty. The difference in quadrature of the CRDS uncertainty and the system uncertainty (determined from GTI) gives an estimate of the uncertainty arising on the preparation side of the system (Table 5). We find that uncertainty on the preparation side of the system accounts for most of the system uncertainty. This highlights the importance of limiting mixing in the system and achieving high-quality depth registration measurements.

As a final analysis using GTI, the reproducibility of GTI-1cm CRDS-CFA data and 1 cm discrete CRDS data are compared. Both are analyzed using a Picarro L2130-*i,* but the exact conditions of measurement are different (e.g. CFA ice stick melting vs. discrete sample injection). A scatter plot and linear regression of the two variables gives a slope, y-intercept, and R^2 value (Figure 8). The coefficient of determination values (R^2) for δD and $\delta^{18}O$ are 0.99 and 1.00, respectively, while dxs remains inherently more difficult to measure with an R^2 value of 0.88. Because this test shows the comparison of seven GTI sticks analyzed on CRDS-CFA compared with a single ice stick measured discretely on CRDS, the R^2 values represents the reproducibility of the average of seven ice sticks vs. a single ice stick carried out under changed conditions of measurement. We explore the reproducibility of sets of single ice sticks for IRMS and CRDS in the following section.

3.2 WAIS Divide Ice Core Tests

The reproducibility of traditional IRMS discrete measurements and CRDS-CFA measurements (both analyzed at the INSTAAR SIL) was tested on the WAIS Divide Ice Core (WDC) over depths of ~212-222 meters (Figure 9). The discrete samples (3 cm cuts) were measured using a uranium reduction technique for δD (Vaughn et al., 1998) and a CO_2/H_2O equilibration method for $\delta^{18}O$ (Epstein; 1953; Craig et al., 1963). We find that the amplitude of the δ signal between the IRMS and CRDS-CFA techniques is nearly identical, although with an occasional offset in δD of 3-4 ‰ and $\delta^{18}O$ of 0.4-0.5 ‰. The offsets in δD and $\delta^{18}O$ do not always occur over the same interval of ice. One possibility is that the standard water calibration on the IRMS instruments was offset relative to the CRDS for some sample groups, which would account for the occasional offset in δD and $\delta^{18}O$ values while retaining the same signal amplitude. Furthermore, if the calibrations for δD and $\delta^{18}O$ were offset in different intervals of ice, this could possibly cause the IRMS dxs values to be negative. Indeed, the dxs values in the IRMS samples are decreased and more negative over the ten-meter section as compared to CRDS-CFA, sometimes with offsets of up to 7‰. Another possible explanation for negative dxs values is that there was fractionation within some of the discrete IRMS sample vials over time.

A second WDC inter-lab reproducibility test was performed between high-resolution CRDS-CFA measurements and low-resolution discrete CRDS measurements (Figure 9). The low-res data were measured at the University of Washington using a Picarro 2120-*i* at ~50 cm increments (Steig et al., 2013). To determine inter-lab reproducibility, we average the high-resolution CRDS-CFA data to the exact low-resolution discrete CRDS increments; we refer to this as “down-sampling”.

Atmos. Meas. Tech. Discuss., doi:10.5194/amt-2016-118, 2016
Manuscript under review for journal Atmos. Meas. Tech.
Published: 26 July 2016

Over a depth of ~212-222 meters, scatter plot comparisons of the down-sampled high-res data and low-res measurements have R^2 values for δD, $\delta^{18}O$, and dxs of 0.99, 0.99, and 0.29, respectively. The combination of the above results lead to the following conclusions: 1) The δD and $\delta^{18}O$ data is reproducible between traditional IRMS and CRDS-CFA techniques, although with an occasional offset in magnitude but not amplitude. We suggest, but cannot prove, that the offset is due to standard water calibration difficulties using IRMS, or due to out-dated sample storage techniques that introduced additional fractionation in the IRMS samples. Both of these scenarios could result in negative dxs values. In any case, we have shown that inter-lab CRDS measurements of δD and $\delta^{18}O$ have high R^2 values (0.99), suggesting that CRDS is the better measurement method or that sample storage techniques for CRDS have been sufficiently improved. 2) The dxs data between IRMS and CRDS-CFA is not reproduced well, either due to the uncertainty introduced by multi-system IRMS measurements or because the discrete samples underwent additional fractionation due to storage procedures. 3) However, the CRDS-CFA analysis of GTI shows that the external precision of dxs has a low average-standard deviation of 0.55 ‰, and when compared with discrete CRDS samples, has a high R^2 value of 0.88. This would suggest that the INSTAAR CRDS-CFA is capable of measuring dxs at high frequencies (annual to multi-year). 4) Yet, inter-lab reproducibility of down-sampled dxs using CRDS is not exact (R^2=0.29), but still within the same range of values between ~0 to 4 per mil. This highlights the fact that both INSTAAR and the University of Washington achieved the same range of measurements using CRDS, whereas IRMS values were often negative. These results suggest that dxs is most reliably measured using CRDS instruments, but that the inherent noise in dxs measurements may make this parameter useful only at longer timescales (decades to centuries) when measured on certain systems. Additional comparison studies at high resolution are necessary to better understand the limitations of dxs.

3.3 South Pole Firn Tests

Measuring firn ice by CFA methods involves additional complexity relative to deep ice. Due to the increased porosity of firn ice, liquid water at the melt head can wick upwards by capillary action through the pore spaces, artificially smoothing the isotopic signal and decreasing signal amplitude. This can, for example, alter frequency analysis calculations or cause the misinterpretation of the size of summer-winter signals. To test the repeatability of CRDS-CFA firn measurements, two identical 1-meter sections from 4, 9, and 29 meters depth in a South Pole firn core are analyzed under the same conditions of measurement (hereafter referred to as South Pole Firn; SPF). The reproducibility of these CRDS-CFA firn measurements is then compared with a third identical 1-meter SPF section discretely sampled at 1 cm increments using a Picarro L2130-*i* (Figure 10).

Based upon a steady-state Herron and Langway density model (Herron and Langway, 1980), the SPF sticks have estimated densities of 340, 386, and 562 kg/m^3 at depths of 4, 9, and 29 meters, respectively (assuming an average accumulation rate of 0.085 m/yr, average temperature of -50°C, average snow density in the top 2 meters of 300 kg/m^3, and pore-close off density

Atmos. Meas. Tech. Discuss., doi:10.5194/amt-2016-118, 2016
Manuscript under review for journal Atmos. Meas. Tech.
Published: 26 July 2016

of 804.3 kg/m^3). For comparison, the density of snow at the surface of the WAIS Divide ice core is ~370 kg/m^3. Because of the low-density SPF sticks, the melt rate was increased from 2.5 cm/min to 4.4 cm/min to prevent wicking during this experiment. We observed that no wicking occurred during the melting process.

The data show that a loss in δD amplitude not surpassing 11% occurred in the CRDS-CFA data relative to the discretely sampled data, while maximum depth registration offsets were 4 cm, <0.5 cm, and <0.5cm at 4, 9, and 29 m depth, respectively. At 4 meters depth, the phase of the CRDS-CFA and discrete δD signal is offset by about 3 cm over the last ~60 cm of the SPF section, which is likely related to imprecise depth registration on the CRDS-CFA due to the increased melt rate or unobserved wicking. At 29 meters depth, CRDS-CFA δD measurements are anomalously higher than discrete measurements in the first 20 cm. The dxs values for the CRDS-CFA and 1 cm discrete signals have the same pattern and range of values, except for small offsets in the last ~60 cm of the 4-meter depth section and again at ~9.30 and ~9.55 meters. The ability to analyze the firn samples was likely improved due to long storage times that allowed the ice sticks to sinter, increasing the structural integrity of the samples. We have found in other subsequent experiments that short storage times causes low-density firn sticks to collapse when placed vertically in the CFA system, introducing large uncertainty in depth registration that is essentially unusable. In any case, we do not find that our CFA results are of high-enough quality for firn samples, and suggest discrete measurements are a better option throughout the firn column.

4 Conclusions

We have presented a high-resolution continuous flow analysis (CFA) system based on cavity ring down spectroscopy technology (CRDS) that is specifically designed for water isotope analysis of ice cores. The CFA system converts ~1 m ice sticks into a continuous liquid water stream, which is then vaporized and analyzed on a CRDS instrument. The full system builds from previous water isotope CFA studies (Gkinis et al., 2010; 2011; Maselli et al., 2012; Emanuelsson et al., 2015) and includes novel improvements to the ice delivery mechanism and the melt head.

Based on our experiments, we have developed a number of new techniques for quantifying system performance within a CRDS-CFA system. For such systems, the uncertainty of an isotopic measurement depends both on analytic uncertainty and on uncertainty introduced from depth registration of the ice core. By analyzing identical ice sticks from the same depth in an ice core (we suggest at least five 1 m ice sticks), a system uncertainty can be determined that includes both analytic uncertainty and depth registration uncertainty. This test is critical for CRDS-CFA systems, as the repeatability of results of identical ice stick measurements will be slightly offset in depth due to uncertainty in the laser measurement device and small perturbations in melt rate. These uncertainties were not present in isotope ratio mass spectrometry (IRMS) because the discrete measurements had a known and unvarying depth registration. We also outline steps for determining system mixing

Atmos. Meas. Tech. Discuss., doi:10.5194/amt-2016-118, 2016
Manuscript under review for journal Atmos. Meas. Tech.
Published: 26 July 2016

Atmospheric Measurement Techniques Discussions

lengths that quantify isotopic signal attenuation introduced by CRDS-CFA. The mixing length value is determined by measuring step-changes in isotopically homogenous ice sticks fabricated in the laboratory; we have suggested a modified approach to the mixing length calculation using a skew normal probability density function rather than a normal probability density function. In a perfectly functioning system, an isotopic step-change would instantaneously register, but in practice the CRDS-CFA system records a delayed and isotopically-mixed response. For both system uncertainty and system mixing length, we outline new techniques that separate the liquid and gas components of these variables. These separation techniques are useful for isolating the portion of a CRDS-CFA system that requires refinement to improve measurement uncertainty. Finally, we suggest a new correction for the isotopic mixing that occurs between ice core melt water and the standard water that precedes the ice core melt sequence. For a 3,000 m ice core, this correction saves up to 25 meters worth of data that would otherwise need to be discarded.

In tests of identical ice samples, we find two difficulties. First, identical firn ice sticks measured on CRDS-CFA are repeated reasonably well, but exhibit offsets as large as ~4 cm in depth and signal attenuation of 11%. For studies that require precise sampling, we recommend discrete sampling of the firn column. Second, inter-lab reproducibility of deuterium excess (dxs) using CRDS-CFA and discrete CRDS are not coherent at the highest frequencies (annual to multi-year). However, dxs measurements can clearly be interpreted at high frequencies on the CRDS-CFA system presented in this study, demonstrated by tests of replicate Greenland ice sticks. This prompts us to suggest additional investigations as to why inter-lab dxs measurements are not better correlated.

The overall results of this study for CRDS-CFA relative to IRMS show an improvement in δD uncertainty (0.55 vs. 1.0 ‰), similar uncertainty in $\delta^{18}O$ (0.09 vs. 0.10 ‰), and a substantial improvement in the uncertainty of dxs (0.55 vs. 1.3 ‰). For a section of ice in the WAIS Divide ice core around 215 meters depth, the average annual signal (i.e. the difference in maximum summer and minimum winter values) for δD, $\delta^{18}O$, and dxs is about 20.0, 2.5, and 4.0 ‰, respectively. This corresponds to a CRDS-CFA signal-to-noise ratio for δD, $\delta^{18}O$, and dxs of about 36, 28, and 7, respectively. In comparison to other water isotope CFA studies, δD and $\delta^{18}O$ uncertainty values for Gkinis et al. (2011) was better slightly than 0.5 and 0.1 ‰, respectively, and for Maselli et al. (2012) was 0.3 and greater than 0.1 ‰, respectively, but at twice the run speed as this study. Emanuelsson et al. (2015) quotes precision uncertainty values based on Allen deviation values after 1.2 hours as 0.13 and 0.17 ‰, respectively. Unlike prior studies, the uncertainty values cited in this paper (termed “system uncertainty”) have the added benefit of including both the analytical uncertainty and depth registration uncertainty. We suggest that future CFA studies utilize the system uncertainty approach, as it is most representative of the total uncertainty introduced by CRDS-CFA systems into water isotope measurements.

Atmos. Meas. Tech. Discuss., doi:10.5194/amt-2016-118, 2016
Manuscript under review for journal Atmos. Meas. Tech.
Published: 26 July 2016

Atmospheric Measurement Techniques Discussions

References

Allan, D. W. (1966). Statistics of atomic frequency standards. *Proceedings of the IEEE*, 54(2), 221-230.

Alley, R. B. (2000). Ice-core evidence of abrupt climate changes. *Proceedings of the National Academy of Sciences*, 97(4), 1331-1334.

Azzalini, A., & Dalla Valle, A. (1996). The multivariate skew-normal distribution. Biometrika, 83(4), 715-726.

Bigeleisen, J., Perlman, M. L., & Prosser, H. C. (1952). Conversion of hydrogenic materials to hydrogen for isotopic analysis. *Analytical Chemistry*, 24(8), 1356-1357.

Bigler, M., Svensson, A., Kettner, E., Vallelonga, P., Nielsen, M. E., & Steffensen, J. P. (2011). Optimization of high-resolution continuous flow analysis for transient climate signals in ice cores. *Environmental Science & Technology*, 45(10), 4483-4489.

Bond, G. C. (1968). Catalysis by metals. *Annu. Rep. Prog. Chem., Sect. A. Gen. Phys and Inorg. Chem.,* 65, 121-128.

Brand, W. A., Geilmann, H., Crosson, E. R., & Rella, C. W. (2009). Cavity ring‐down spectroscopy versus high‐temperature conversion isotope ratio mass spectrometry; a case study on δ^2H and $\delta^{18}O$ of pure water samples and alcohol/water mixtures. *Rapid Communications in Mass Spectrometry*, 23(12), 1879-1884.

Coleman, M. L., Shepherd, T. J., Durham, J. J., Rouse, J. E., & Moore, G. R. (1982). Reduction of water with zinc for hydrogen isotope analysis. *Analytical Chemistry*, 54(6), 993-995.

Coplen, T. B., Wildman, J. D., & Chen, J. (1991). Improvements in the gaseous hydrogen-water equilibration technique for hydrogen isotope-ratio analysis. *Analytical Chemistry*, 63(9), 910-912.

Craig, H., Gordon, L. I., & Horibe, Y. (1963). Isotopic exchange effects in the evaporation of water: 1. Low‐temperature experimental results. *Journal of Geophysical Research*, 68(17), 5079-5087.

Crosson, E. R. (2008). A cavity ring-down analyzer for measuring atmospheric levels of methane, carbon dioxide, and water vapor. *Applied Physics B*, 92(3), 403-408.

Cuffey, K. M., & Steig, E. J. (1998). Isotopic diffusion in polar firn: implications for interpretation of seasonal climate parameters in ice-core records, with emphasis on central Greenland. *Journal of Glaciology*, 44(147), 273-284.

Dansgaard, W. (1964). Stable isotopes in precipitation. *Tellus*, 16(4), 436-468.

Dansgaard, W., White, J. W. C., & Johnsen, S. J. (1989). The abrupt termination of the Younger Dryas climate event. *Nature*, 339, 532-534.

Dansgaard, W. (2005). Frozen Annals – Greenland Icecap Research. Niels Bohr Institute, *Narayana Press*, Odder, Denmark, www.narayanapress.dk. ISBN: 87-990078-0-0. 124 p.

Emanuelsson, B. D., Baisden, W. T., Bertler, N. A. N., Keller, E. D., & Gkinis, V. (2015). High-resolution continuous-flow analysis setup for water isotopic measurement from ice cores using laser spectroscopy. *Atmospheric Measurement Techniques*, 8(7), 2869-2883.

Epstein, S., Buchsbaum, R., Lowenstam, H. A., & Urey, H. C. (1953). Revised carbonate-water isotopic temperature scale.

Atmos. Meas. Tech. Discuss., doi:10.5194/amt-2016-118, 2016
Manuscript under review for journal Atmos. Meas. Tech.
Published: 26 July 2016

Atmospheric Measurement Techniques Discussions

Geological Society of America Bulletin, 64(11), 1315-1326.

Gkinis, V., Popp, T. J., Johnsen, S. J., & Blunier, T. (2010). A continuous stream flash evaporator for the calibration of an IR cavity ring-down spectrometer for the isotopic analysis of water. *Isotopes in environmental and health studies*, 46(4), 463-475.

Gkinis, V., Popp, T.J., Blunier, T., Bigler, M., Schupbach, S., Kettner, E., Johnsen, S.J. (2011). Water isotopic ratios from a continuously melted ice core sample. *Atmos. Meas. Tech*. 4, 2531–2542.

Grootes, P. M., Stuiver, M., White, J. W. C., Johnsen, S., & Jouzel, J. (1993). Comparison of oxygen isotope records from the GISP2 and GRIP Greenland ice cores. *Nature* 366(6455):552–4.

Gupta, P., Noone, D., Galewsky, J., Sweeney, C., & Vaughn, B. H. (2009). Demonstration of high‐precision continuous measurements of water vapor isotopologues in laboratory and remote field deployments using wavelength‐scanned cavity ring‐down spectroscopy (WS‐CRDS) technology. *Rapid communications in mass spectrometry*, 23(16), 2534-2542.

Herron, M. M., & Langway Jr, C. C. (1980). Firn densification: an empirical model. *Journal of Glaciology*, 25, 373-385.

Huber, C., & Leuenberger, M. (2003). Fast high‐precision on‐line determination of hydrogen isotope ratios of water or ice by continuous‐flow isotope ratio mass spectrometry. *Rapid communications in mass spectrometry*, 17(12), 1319-1325.

Huber, C., & Leuenberger, M. (2005). On-line systems for continuous water and gas isotope ratio measurements†. *Isotopes in environmental and health studies*, 41(3), 189-205.

Johnsen, S. J., Dahl‐Jensen, D., Gundestrup, N., Steffensen, J. P., Clausen, H. B., Miller, H., Masson-Delmotte, V., Sveinbjörnsdottir, A. E., & White, J. (2001). Oxygen isotope and palaeotemperature records from six Greenland ice‐core stations: Camp Century, Dye‐3, GRIP, GISP2, Renland and NorthGRIP. *Journal of Quaternary Science*, 16(4), 299-307.

Jouzel, J., & Merlivat, L. (1984). Deuterium and oxygen 18 in precipitation: modeling of the isotopic effects during snow formation. *Journal of Geophysical Research: Atmospheres* (1984–2012), 89(D7), 11749-11757.

Jouzel, J., Alley, R. B., Cuffey, K. M., Dansgaard, W., Grootes, P., Hoffmann, G., Johnsen, S. J., Koster, R. D., Peel, D., Shuman, A., Stievenard, M., Stuiver, M., & White, J. (1997). Validity of the temperature reconstruction from water isotopes in ice cores. J*ournal of Geophysical Research: Oceans* (1978–2012), 102(C12), 26471-26487.

Kavanaugh, J. L., & Cuffey, K. M. (2003). Space and time variation of δ18O and δD in Antarctic precipitation revisited. *Global Biogeochemical Cycles*, 17(1).

Kerstel, E. T., Van Trigt, R., Reuss, J., & Meijer, H. A. J. (1999). Simultaneous determination of the 2H/1H, 17O/16O, and 18O/16O isotope abundance ratios in water by means of laser spectrometry. *Analytical chemistry*, 71(23), 5297-5303.

Lin, Y., Clayton, R. N., & Gröning, M. (2010). Calibration of δ17O and δ18O of international measurement standards–VSMOW, VSMOW2, SLAP, and SLAP2. *Rapid Communications in Mass Spectrometry*, 24(6), 773-776.

Lis, G., Wassenaar, L. I., & Hendry, M. J. (2008). High-precision laser spectroscopy D/H and 18O/16O measurements of microliter natural water samples. *Analytical Chemistry*, 80(1), 287-293.

Maselli, O. J., Fritzsche, D., Layman, L., McConnell, J. R., & Meyer, H. (2013). Comparison of water isotope-ratio determinations using two cavity ring-down instruments and classical mass spectrometry in continuous ice-core analysis. *Isotopes in environmental and health studies*, 49(3), 387-398.

Mook, W. (2000). Environmental Isotopes in the Hydrological Cycle. IHP-V Technical Documents in Hydrology No. 39. *UNESCO/IAEA*: Paris/Vienna.

Osterberg, E. C., Handley, M. J., Sneed, S. B., Mayewski, P. A., & Kreutz, K. J. (2006). Continuous ice core melter system with discrete sampling for major ion, trace element, and stable isotope analyses. *Environmental science & technology*, 40(10), 3355-3361.

Petit, J.R., Jouzel, J., Raynaud, D., Barkov, N.I., Barnola, J.M., Basile, I., Bender, M., Chappellaz, J., Davis, M., Delaygue, G. & Delmotte, M. (1999). Climate and atmospheric history of the past 420,000 years from the Vostok ice core, Antarctica. *Nature*, 399(6735), 429-436.

Rhodes, R. H., Faïn, X., Stowasser, C., Blunier, T., Chappellaz, J., McConnell, J. R., Romanini, D., Mitchell, L. E. & Brook, E. J. (2013). Continuous methane measurements from a late Holocene Greenland ice core: Atmospheric and in-situ signals. *Earth and Planetary Science Letters*, 368, 9-19.

Röthlisberger, R., Bigler, M., Hutterli, M., Sommer, S., Stauffer, B., Junghans, H. G., & Wagenbach, D. (2000). Technique for continuous high-resolution analysis of trace substances in firn and ice cores. *Environmental Science & Technology*, 34(2), 338-342.

Steig, E. J., Ding, Q., White, J. W. C., Kuttel, M., Rupper, S. B., Neumann, T. A., Neff, P. D., Gallant, A. J. E., Mayewski, P. A., Taylor, K. C., Hoffmann, G., Dixon, D. A., Schoenemann, S. W., Markle, B. R., Fudge, T. J., Schneider, D. P., Schauer, A. J., Teel, R. P., Vaughn, B. H., Burgener, L., Williams, J., & Korotkikh, E. (2013), Recent climate and ice-sheet changes in West Antarctica compared with the past 2,000 years, *Nature Geoscience*, 6(5), 372–375.

Steig, E. J., Gkinis, V., Schauer, A. J., Schoenemann, S. W., Samek, K., Hoffnagle, J., ... & Tan, S. M. (2014). Calibrated high-precision 17 O-excess measurements using cavity ring-down spectroscopy with laser-current-tuned cavity resonance. *Atmospheric Measurement Techniques*, 7(8), 2421-2435.

Vaughn, B. H., White, J. W. C., Delmotte, M., Trolier, M., Cattani, O., & Stievenard, M. (1998). An automated system for hydrogen isotope analysis of water. *Chemical Geology*, 152(3), 309-319.

WAIS Divide Project Members. (2015). Precise interpolar phasing of abrupt climate change during the last ice age. *Nature*, 520(7549), 661-665.

Atmos. Meas. Tech. Discuss., doi:10.5194/amt-2016-118, 2016
Manuscript under review for journal Atmos. Meas. Tech.
Published: 26 July 2016

Atmospheric Measurement Techniques Discussions

Acknowledgements

This work was supported by US National Science Foundation (NSF) grants 0537930, 0537593, 1043092 and 1043167. The authors would like to thank all field crew, laboratory staff, students, and principal investigators involved with the project. Field and logistical activities were managed by the WAIS Divide Science Coordination Office at the Desert Research Institute, Reno, NE, USA and the University of New Hampshire, USA (NSF grants 0230396, 0440817, 0944266, and 0944348). The National Science Foundation Division of Polar Programs funded the Ice Drilling Program Office (IDPO), the Ice Drilling Design and Operations (IDDO) group, the National Ice Core Laboratory (NICL), the Antarctic Support Contractor, and the 109th New York Air National Guard. Finally, we would like to thank the Centre for Ice and Climate at the Neils Bohr Institute, University of Copenhagen for support in the design of the analysis system used in this study.

Atmos. Meas. Tech. Discuss., doi:10.5194/amt-2016-118, 2016
Manuscript under review for journal Atmos. Meas. Tech.
Published: 26 July 2016

Atmospheric Measurement Techniques Discussions

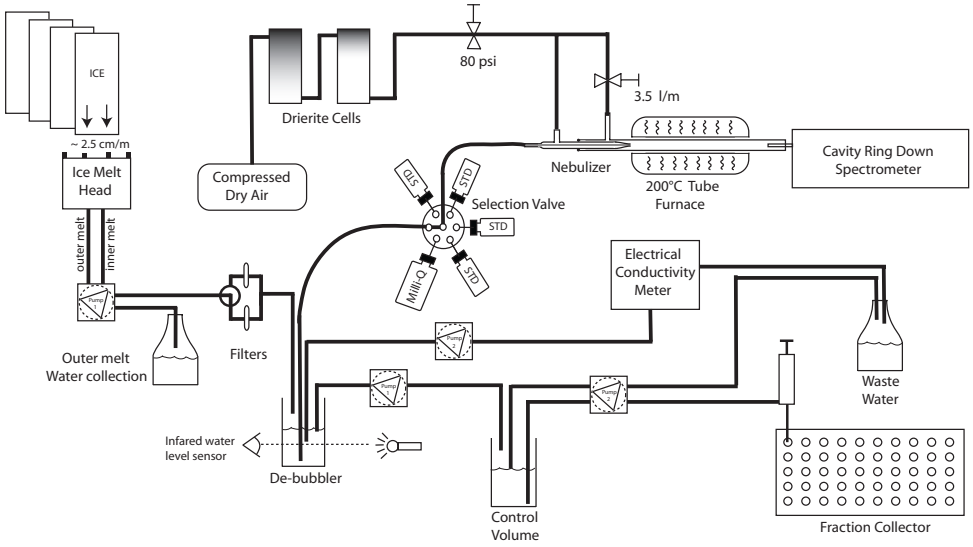

Figure 1: The INSTAAR CRDS-CFA system, showing sample flow from the ice melt head through the filter block and debubbler and on to the Valco stream selection valve, nebulizer, furnace and the Picarro L-2130-i CRDS instrument.

5

Atmos. Meas. Tech. Discuss., doi:10.5194/amt-2016-118, 2016
Manuscript under review for journal Atmos. Meas. Tech.
Published: 26 July 2016

Atmospheric Measurement Techniques Discussions

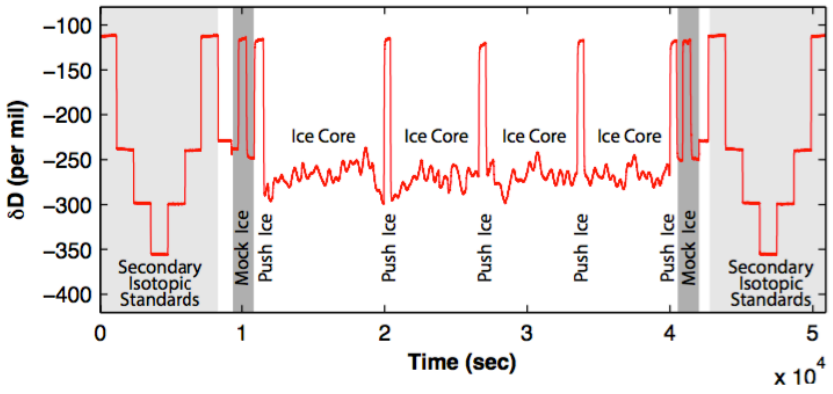

Figure 2: A typical CRDS-CFA melt day consisting of the analysis of 12 meters of ice core sticks from the WDC. The light grey regions show the analysis of four calibrated secondary isotopic standards. The dark grey regions show the analysis of mock ice. The prominent white region shows the analysis of ice core sticks separated by short sections of push ice every fourth ice stick.

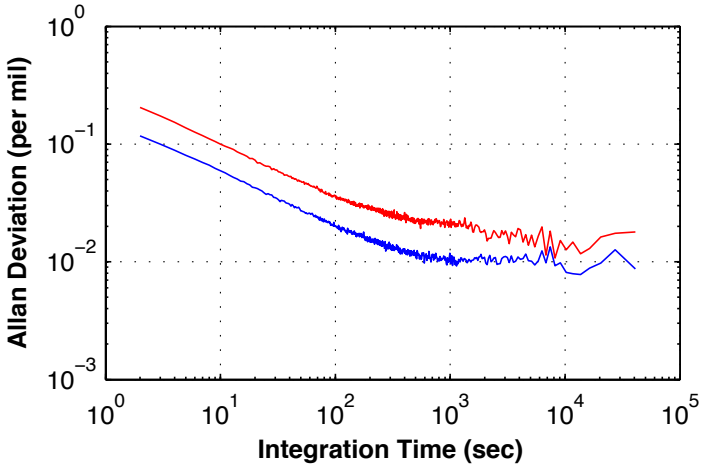

Figure 3: A 7-hour analysis of Allan deviation for δD (red) and $\delta^{18}O$ (blue) on the CRDS-CFA using isotopically homogenous water vapor.

Atmos. Meas. Tech. Discuss., doi:10.5194/amt-2016-118, 2016
Manuscript under review for journal Atmos. Meas. Tech.
Published: 26 July 2016

Atmospheric Measurement Techniques Discussions

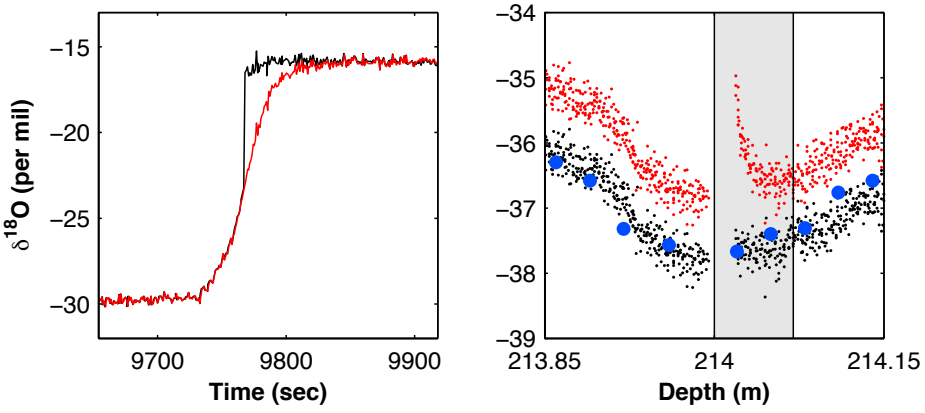

Figure 4: Mixing corrections for mock ice (left) and the beginning of an ice core section (right). The ice core mixing correction is based upon a known step-function change defined by the mock ice, from which mixing coefficients are determined. Red represents raw uncorrected isotopic data with no memory correction, black represents VSMOW-VSLAP2 corrected data with the memory correction applied, blue dots represent 3 cm IRMS discrete samples, and the grey region represents the time and depth range of corrected data that would otherwise be discarded. Note that the time variable represents the amount of run time on a given day.

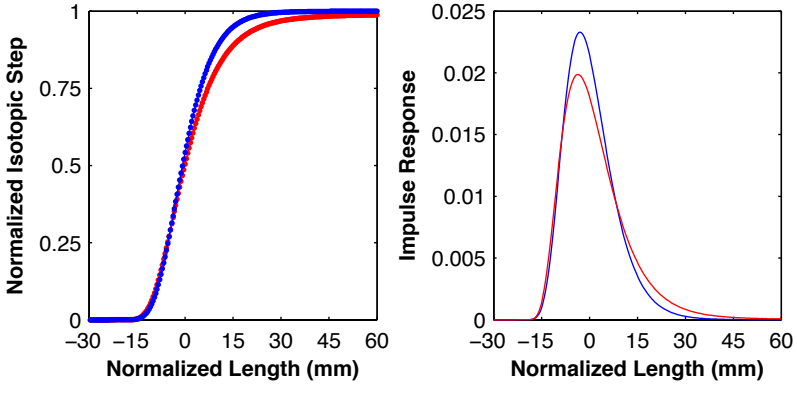

Figure 5: The log-log CDF transfer functions (left) and skew normal impulse response functions (right) of the CRDS-CFA system for δD (red) and $\delta^{18}O$ (blue). The functions are derived from a normalized mock ice isotopic step change in δD from -240‰ to -120‰. The normalized length scale is calculated using an average melt rate of 2.5 cm per minute.

Atmos. Meas. Tech. Discuss., doi:10.5194/amt-2016-118, 2016
Manuscript under review for journal Atmos. Meas. Tech.
Published: 26 July 2016

Atmospheric Measurement Techniques Discussions

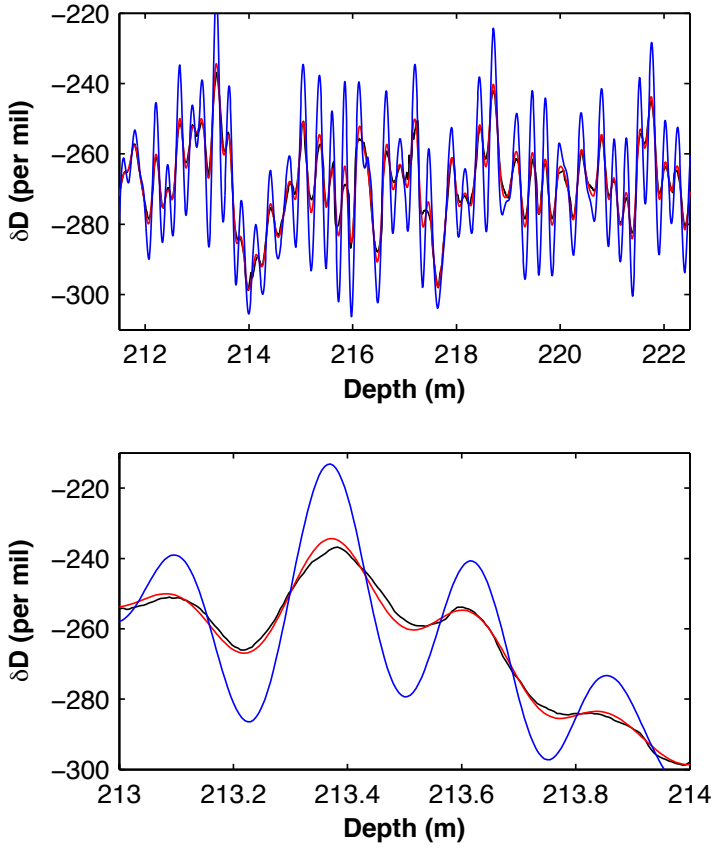

Figure 6: A comparison of the WAIS Divide ice core δD signal measured on the CRDS-CFA system (black), the CRDS-CFA mixing corrected isotopic signal using $\sigma_{mock\ ice}$ of 0.8 cm (red), and a correction for a typical West Antarctic diffusion value of 6.5 cm (blue), which represents diffusional processes occurring naturally in the ice sheet (see Figure 6 of Cuffey and Steig, 1998). The mixing introduced by the CRDS-CFA is only a fraction of the diffusion occurring naturally in the ice sheet.

Atmos. Meas. Tech. Discuss., doi:10.5194/amt-2016-118, 2016
Manuscript under review for journal Atmos. Meas. Tech.
Published: 26 July 2016

Atmospheric Measurement Techniques Discussions

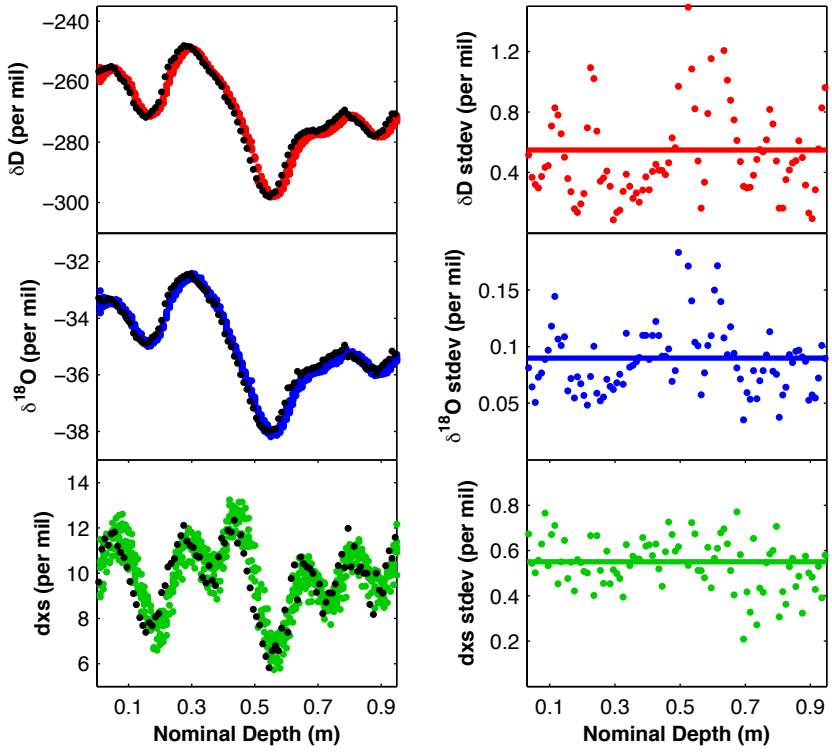

Figure 7: Greenland test ice (GTI) for a nominal 1-meter section. In the left column, seven GTI sticks measured on the CRDS-CFA system averaged to 1 cm increments for δD (red dots), $\delta^{18}O$ (blue dots), and dxs (green dots) compared with discrete 1 cm samples (black dots) measured on a Picarro L2130-i. In the right column, the standard deviation of seven GTI values is taken at each 1 cm increment (red, blue, and green dots). The average standard deviation is shown by the horizontal line, which represents the system uncertainty (1σ) for δD, $\delta^{18}O$, and dxs.

Atmos. Meas. Tech. Discuss., doi:10.5194/amt-2016-118, 2016
Manuscript under review for journal Atmos. Meas. Tech.
Published: 26 July 2016

Atmospheric Measurement Techniques Discussions

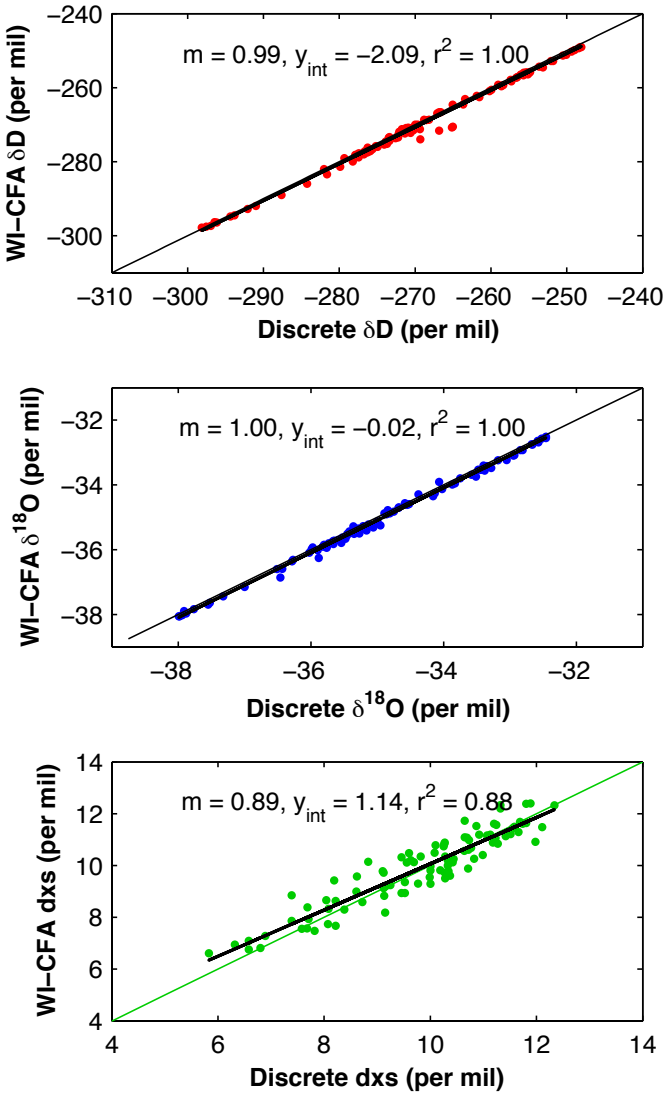

Figure 8: Scatter plots of Greenland test ice (GTI) comparisons of CRDS-CFA vs. CRDS-discrete data. Seven GTI sticks were analyzed on the CRDS-CFA data, down-sampled to 1 cm, and averaged. The discrete data were sampled at 1 cm and analyzed on a separate Picarro L-2130i. The black line is the best-fit linear regression.

5

Atmos. Meas. Tech. Discuss., doi:10.5194/amt-2016-118, 2016
Manuscript under review for journal Atmos. Meas. Tech.
Published: 26 July 2016

Atmospheric Measurement Techniques Discussions

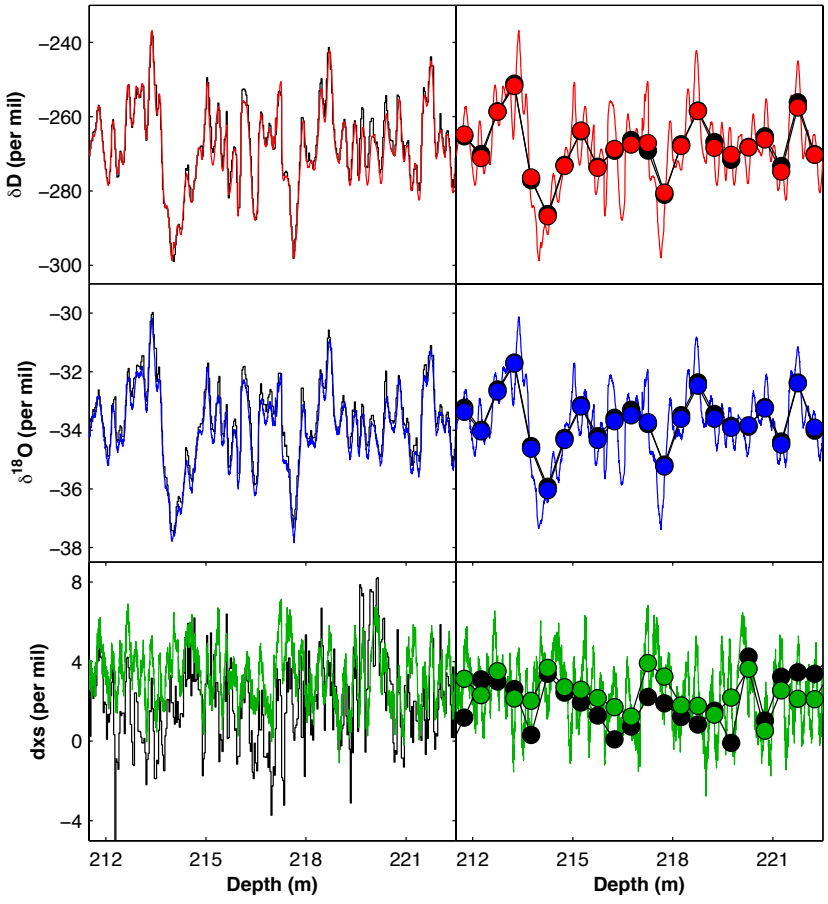

Figure 9: Data from the WDC over a depth range of ~212-222 meters. In the left column, high-resolution CRDS-CFA data for δD (red line), $\delta^{18}O$ (blue line), and dxs (green line) compared with traditional high-resolution IRMS discrete samples (black lines). In the right column, comparison of high-resolution CRDS-CFA data (red, blue, and green lines), low-resolution University of Washington CRDS discrete samples (black dots), and down-sampled CRDS-CFA data (red, blue, and green dots).

Atmos. Meas. Tech. Discuss., doi:10.5194/amt-2016-118, 2016
Manuscript under review for journal Atmos. Meas. Tech.
Published: 26 July 2016

Atmospheric Measurement Techniques Discussions

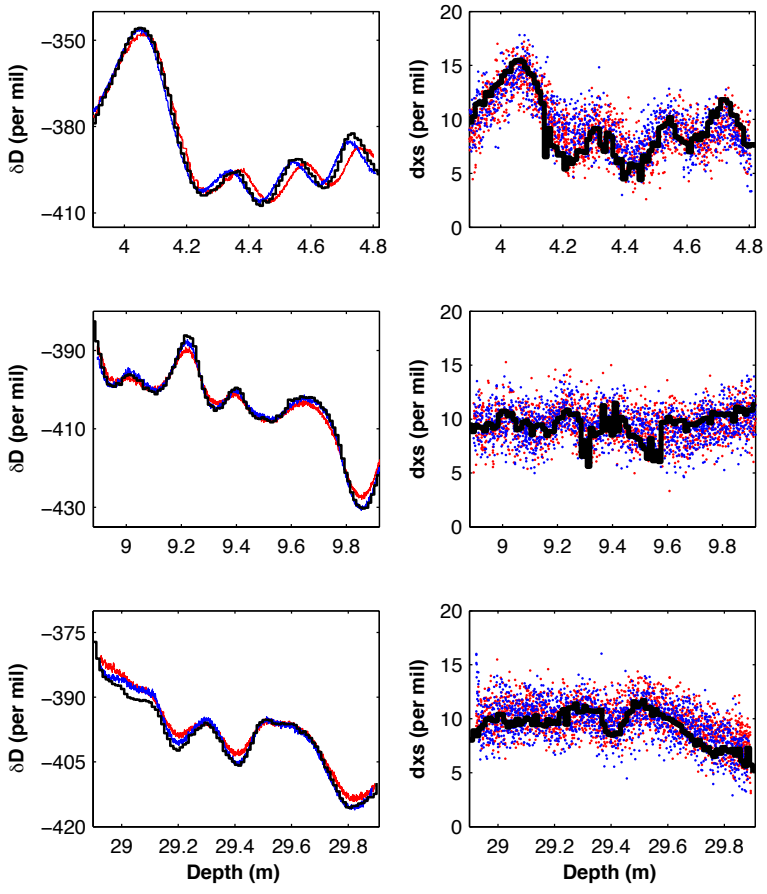

Figure 10: Replicate SPF ice measurements of δD and dxs at depths of ~4, 9, and 29 m, corresponding to densities of 340, 386, and 562 kg/m^3, respectively. The red and blue data are from SPF sticks analyzed on the CRDS-CFA system and the black data are 1 cm discrete samples analyzed on a separate Picarro L2130-i.

Atmos. Meas. Tech. Discuss., doi:10.5194/amt-2016-118, 2016
Manuscript under review for journal Atmos. Meas. Tech.
Published: 26 July 2016

Atmospheric Measurement Techniques Discussions

Table 1: List of abbreviations used in this paper.

Type	Name	Abbreviation
Ice Core Drilling Sites	West Antarctic Ice Sheet Divide Ice Core	WDC
	South Pole Ice Core	SPICE
Measurement Devices	Isotope Ratio Mass Spectrometry	IRMS
	Laser Absorption Spectrometers	LAS
	Continuous Flow Analysis	CFA
	Cavity Ring-Down Laser Spectroscopy	CRDS
	Off-Axis Integrated Cavity Output Laser Spectroscopy	OA-ICOS
Water Isotope Standards	International Atomic Energy Agency	IAEA
	Vienna Standard Mean Ocean Water	VSMOW
	Standard Light Antarctic Precipitation	SLAP
	Greenland Ice Sheet Precipitation	GISP
	Boulder Standard Water	BSW
	Antarctic Standard Water	ASW
	Greenland Standard Water	GSW
	Polar Standard Water	PSW
System Performance	Allan Variance	AVAR
	Cumulative Distribution Function	CDF
	Secondary Water Isotope Standards	SWS
	Greenland Test Ice	GTI
	Isotopically Homogenous Water	IHW
	South Pole Firn	SPF

5

Atmos. Meas. Tech. Discuss., doi:10.5194/amt-2016-118, 2016
Manuscript under review for journal Atmos. Meas. Tech.
Published: 26 July 2016

Atmospheric Measurement Techniques Discussions

Table 2: Water isotope standards in units of per mil (‰). The secondary standards (BSW, ASW, GSW, and PSW) were calibrated to primary standards (VSMOW2, SLAP2, and GISP) in March 2010. The primary standards are reported with errors given by the IAEA. The secondary standards are reported with uncertainty given by the average standard deviation (1σ) of multiple isotopic determinations across multiple analysis platforms (IRMS and CRDS).

Standards	δD	δD uncertainty	$\delta^{18}O$	$\delta^{18}O$ uncertainty
VSMOW2	0	0.3	0	0.02
SLAP2	-427.5	0.3	-55.5	0.02
GISP	-189.5	1.2	-24.76	0.09
BSW	-111.8	0.2	-14.19	0.02
ASW	-239.3	0.3	-30.35	0.04
GSW	-298.7	0.2	-38.09	0.03
PSW	-355.6	0.2	-45.43	0.05

Table 3: Selected Allan deviation values (‰) for a 7-hour analysis of isotopically homogenous water on the CRDS-CFA system.

Integration Time (sec)	δD	$\delta^{18}O$
10	0.1	0.063
60	0.045	0.026
600	0.022	0.01
3600	0.017	0.009

Atmos. Meas. Tech. Discuss., doi:10.5194/amt-2016-118, 2016
Manuscript under review for journal Atmos. Meas. Tech.
Published: 26 July 2016

Atmospheric Measurement Techniques Discussions

Table 4: Mixing lengths determined from mock ice step changes ($\sigma_{mock\ ice}$) and from secondary isotopic standards step changes (σ_{SWS}). The difference in quadrature of $\sigma_{mock\ ice}$ and σ_{SWS} is the amount of mixing occurring in the liquid phase of the CRDS-CFA system (σ_{LQD}). Mixing length values for both skew and normal impulse response functions are given in seconds and in meters (in parentheses), based on a melt rate of 2.5 cm/min.

	σ_{SWS}		$\sigma_{mock\ ice}$		σ_{LQD}	
Fit Type	**δD**	**$\delta^{18}O$**	**δD**	**$\delta^{18}O$**	**δD**	**$\delta^{18}O$**
Skew	10.3	9.6	18.7	17.7	15.6	14.9
	(0.004)	(0.004)	(0.008)	(0.007)	(0.007)	(0.006)
Normal	10.2	9.4	19.1	17.4	16.1	14.6
	(0.004)	(0.004)	(0.008)	(0.007)	(0.007)	(0.006)

Table 5: The isotopic measurement uncertainty (1σ) of varying parts of the CRDS-CFA system (‰). The difference in quadrature of the system uncertainty derived from GTI (System) and that arising from the Picarro instrument (CRDS) gives an estimate of the uncertainty introduced on the preparation side of the system (PREP). The preparation uncertainty includes all uncertainty except that arising from analysis in the Picarro instrument.

Measurement	System	CRDS	PREP
δD	0.55	0.09	0.54
$\delta^{18}O$	0.09	0.04	0.08
dxs	0.55	0.32	0.45